Article

A Molecular Mechanism for the Chemoselective Hydrogenation of Substituted Nitroaromatics with Nanoparticles of Gold on TiO Catalysts: A Cooperative Effect between Gold and the Support

Merc Boronat, Patricia Concepcin, Avelino Corma, Silvia Gonzlez, Francesc Illas, and Pedro Serna

J. Am. Chem. Soc., **2007**, 129 (51), 16230-16237 • DOI: 10.1021/ja076721g

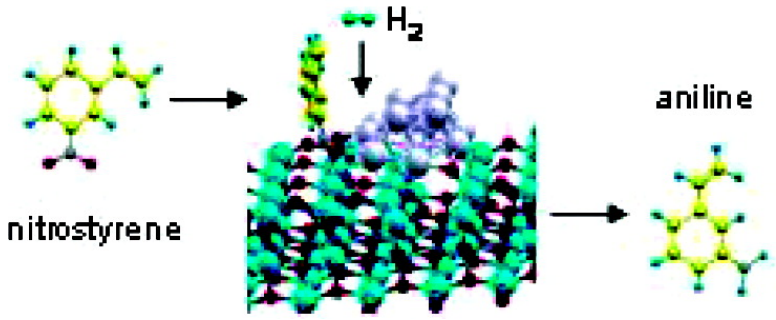

More About This Article

Additional resources and features associated with this article are available within the HTML version:

- Supporting Information
- Links to the 7 articles that cite this article, as of the time of this article download
- Access to high resolution figures
- Links to articles and content related to this article
- Copyright permission to reproduce figures and/or text from this article

View the Full Text HTML

J|A|C|S
ARTICLES
Published on Web 12/01/2007

A Molecular Mechanism for the Chemoselective Hydrogenation of Substituted Nitroaromatics with Nanoparticles of Gold on TiO_2 Catalysts: A Cooperative Effect between Gold and the Support

Mercè Boronat,[†] Patricia Concepción,[†] Avelino Corma,*[,†] Silvia González,[‡] Francesc Illas,[‡] and Pedro Serna[†]

Instituto de Tecnología Química, Universidad Politécnica de Valencia-CSIC, Av. de los Naranjos s/n, 46022 Valencia, Spain, and Departament de Química Física and Institut de Química Teòrica i Computacional, (IQTCUB) Universitat de Barcelona and Parc Científic de Barcelona, C/Martí i Franquès 1, E-08b028 Barcelona, Spain

Received September 14, 2007; E-mail: acorma@itq.upv.es

Abstract: Nanoparticles of gold on TiO_2 are highly chemoselective for the reduction of substituted nitroaromatics, such as nitrostyrene. By combining kinetics and *in situ* IR spectroscopy, it has been found that there is a preferential adsorption of the reactant on the catalyst through the nitro group. IR studies of nitrobenzene, styrene, and nitrostyrene adsorption, together with quantum chemical calculations, show that the nitro and the olefinic groups adsorb weakly on the Au(111) and Au(001) surfaces, and that although a stronger adsorption occurs on low-coordinated atoms in gold nanoparticles, this adsorption is not selective. On the other hand, an energetically and geometrically favored adsorption through the nitro group occurs on the TiO_2 support and in the interface between the gold nanoparticle and the TiO_2 support. Such preferential adsorption is not observed with nanoparticles of gold on silica which, contrary to the Au/TiO_2 catalyst, is not chemoselective for the reduction of substituted nitroaromatic compounds. Therefore, the high chemoselectiviy of the Au/TiO_2 catalyst can be attributed to a cooperation between the gold nanoparticle and the support that preferentially activates the nitro group.

Introduction

Supported gold catalysts have shown interesting possibilities for selective oxidations,[1] carbon−carbon bond formation, and reactions with alkynes and alkenes among others.[2−4] A more modest role has been played by supported gold catalysts for selective hydrogenations. Only in the case of α,β-unsaturated aldehydes such as crotonaldehyde, acroleine, citral, and pent-3-en-2-one[5] is Au supported on ZrO_2 and ZnO able to catalyze the selective hydrogenation of the carbonyl group. However, selectivities are high only at low conversion levels, and gold still cannot compete with supported Pt doped with Sn, or with Pt on CeO_2, for the selective hydrogenation of carbonyls in the presence of C=C double bonds, especially at high levels of conversion.[6,7]

We have recently shown that Au/TiO_2 has unique catalytic behavior for the chemoselective hydrogenation of the nitro group in substituted nitroaromatics.[8] Interestingly, none of the supported Pt catalysts reported up to now could achieve the degree of selectivity of gold, unless other catalytic functions were present in the homogeneous phase.[9] While the unique behavior of gold was clearly demonstrated,[10] why this occurs and which

[†] Universidad Politecnica de Valencia-CSIC.
[‡] Universitat de Barcelona and Parc Científic de Barcelona.

(1) (a) Haruta, M.; Yamada, N.; Kobayashi, T.; Iijima, S. *J. Catal.* **1989**, *115*, 301−309. (b) Landon, P.; Collier, P. J.; Papworth, A. J.; Kiely, C. J.; Hutchings, G. J. *Chem. Commun.* **2002**, 2058−2059. (c) Abad, A.; Concepcion, P.; Corma, A.; Garcia, H. *Angew. Chem., Int. Ed.* **2005**, *44*, 4066−4069. (d) Abad, A.; Almeda, C.; Corma, A.; Garcia, H. *Chem. Commun*. **2006**, 3178−3180. (e) Hayashi, T.; Tanaka, K.; Haruta, M. *J. Catal*. **1998**, *178*, 566−575. (f) Davis, R. J. *Science* **2003**, *301*, 926−927. (g) Hughes, M. D.; et al. *Nature* **2005**, *437*, 1132−1135. (h) Prati, L.; Rossi, M. *Stud. Surf. Sci. Catal*. **1997**, *110*, 509−516. (i) Coluccia, S.; Martra, G.; Porta, F.; Prati, L.; Rossi, M. *Catal. Today* **2000**, *61*, 165−172. (j) Enache, D. I.; Edwards, J. K.; Landon, P.; Solsona-Espriu, B.; Carley, A. F.; Herzing, A. A.; Watanabe, M.; Kiely, C. J.; Knight, D. W.; Hutchings, G. J. *Science* **2006**, *311*, 362−365. (k) Corma, A.; Domine, M. *Chem. Commun.* **2005**, 4042−4044.
(2) (a) Carrettin, S.; Guzman, J.; Corma, A. *Angew. Chem., Int. Ed*. **2005**, *44*, 2242−2245. (b) González-Arellano, C.; Corma, A.; Iglesias, M.; Sánchez, F. *J. Catal*. **2006**, *238*, 497−501. (c) González-Arellano, C.; Abad, A.; Corma, A.; García, H.; Iglesias, M.; Sánchez, F. *Angew. Chem., Int. Ed*. **2007**, *46*, 1536−1538.
(3) Hashmi, A. S. K.; Hutchings, G. *Angew. Chem., Int. Ed*. **2006**, *45*, 7896−7936.
(4) Hashmi, A. S. K. *Chem. Rev*. **2007**, *107*, 3180−3211.
(5) (a) Bailie, J. E.; Hutchings, G. J. *Chem. Commun.* **1999**, 2151−2152. (b) Radnick, J.; Mohr, C.; Claus, P. *Phys. Chem. Chem. Phys*. **2003**, *5*, 172−177. (c) Milone, G.; Tropeano, M. L.; Gulino, G.; Neri, G.; Ingoglia, Q.; Galvano, S. *Chem. Commun.* **2002**, 868−869. (d) Fordham, P.; Besson, M.; Gallezot, P. *Stud. Surf. Sci. Catal*. **1997**, *108*, 429−436.
(6) (a) Concepción, P.; Corma, A.; Silvestre-Albero, J.; Franco, V.; Chane-Ching, J. Y. *J. Am. Chem. Soc*. **2004**, *126*, 5523−5532. (b) Sepúlveda-Escribano, A.; Coloma, F.; Rodriguez-Reinoso, F. *J. Catal*. **1998**, *178*, 649−657. (c) Abid, M.; Touroude, R. *Catal. Lett.* **2000**, *69*, 139−144. (d) Silvestre-Albero, J.; Rodriguez-Reinoso, F.; Sepúlveda-Escribano, A. *J. Catal.* **2002**, *210*, 127−136.
(7) (a) Coloma, F.; Sepúlveda-Escribano, A.; Fierro, J. L. G.; Rodriguez-Reinoso, F. *Appl. Catal. A* **1996**, *148*, 63−80. (b) Margitfalvi, J. L.; Vankó, Gy.; Borbáth, I.; Tompos, A.; Vértes, A. *J. Catal.* **2000**, *190*, 474−477.
(8) Corma, A.; Serna, P. *Science* **2006**, *313*, 332−333.
(9) Siegrist, U.; Baumeister, P.; Blaser, H.-U. *Chem. Ind.* **1998**, *75*, 207−219.

10.1021/ja076721g CCC: $37.00

active sites are involved in the chemoselective reduction of substituted nitroaromatics to the corresponding anilines remain unknown.

In the present work, we have studied, at the molecular level, the interactions between the reactants and the catalyst surface by combining *in situ* IR spectroscopy, realistic quantum chemical modeling, and kinetic experiments. It will be shown that, during nitrostyrene hydrogenation with Au/TiO_2, there is a cooperative effect between gold and TiO_2 such that H_2 is dissociated on Au and nitrostyrene is adsorbed selectively on the support through the nitro group only, especially on the gold atoms located at the boundary between TiO_2 and Au, these very specific adsorption sites being responsible for the high chemoselectivity observed.

Experimental Section

Catalyst and Catalytic Experiments. The Au/TiO_2 and the Au/Fe_2O_3 catalysts, with 1.5 wt % and 4.5 wt % loadings of gold, respectively, were supplied by the World Gold Council (reference catalysts, Type A and D). Other gold catalysts, i.e., 1.5 wt % Au/C and 1.6 wt % Au/SiO_2, were prepared following recently described procedures,[11] the average gold particle size being between 3.5 and 4.0 nm in all cases. Finally, a 2 wt % Pt/TiO_2 catalyst was prepared by the incipient wetness technique using H_2PtCl_6 as platinum precursor. This catalyst was reduced under H_2 flow during 5 h at 200 °C before its use in the reaction.

Catalytic experiments were carried out in 2 mL glass reactors, through the following procedure: First, an appropriate amount of the catalyst is placed into the reactor, together with the reaction mixture (1 mL). The system is then purged with H_2, before heating, in order to completely remove oxygen from the reactor. Under H_2 atmospheric pressure, the reaction mixture is heated at 120 °C with magnetic stirring, and then the pressure is set to 9 bar of H_2, this being the starting reaction time. Aliquots were taken from the reactor at different times and analyzed by GC and MS−GC measurements.

IR Experiments. FTIR spectra were collected with an FTS-40A spectrometer using a quartz cell connected to a vacuum line. The samples were evacuated at 10^{-2} mbar for 20 min prior to the adsorption experiment. Nitrobenzene, styrene, and nitrostyrene were adsorbed at increasing pressures from 0.1 to 20 mbar.

Theoretical Calculations. Density functional calculations were carried out with a series of models of increasing complexity, the final system being sufficiently close to the experimental situation, although still modeling ultra-high-vacuum conditions. Hence, adsorption of nitrostyrene on different Au models—namely, single-crystal Au(111) and Au(001) surfaces, a monatomic row model which contains low-coordinated gold atoms, an isolated Au_{38} nanoparticle, and a Au_{13} nanoparticle supported on TiO_2—has been explicitly considered. Adsorption on the titanium oxide support has also been considered.

The Au(111) and Au(100) were modeled by periodic slabs containing four atomic layers and a vacuum region larger than 20 Å between vertical repeated slabs. Large enough supercells—(4×4) for Au(111) and (3×3) for Au(001)—were used to avoid interaction between the adsorbates. The monatomic row model was constructed from a (5×5) supercell slab model for the Au(111) model with five atomic layers and with two rows and one row missing in the topmost and second layers, respectively. Although the Au monatomic row model (Au_{MAR}) may appear somewhat artificial, it provides an adequate model for low-coordinated Au atoms appearing in stepped surfaces and nanoparticle edges. In the geometry optimizations, the two innermost atomic layers were kept as in the bulk to provide an adequate metallic environment to the topmost layers, which are fully relaxed. As representative of nanoscale Au particles, a Au_{38} cluster (∼1 nm diameter) was placed in a 20 Å × 20 Å × 20 Å cubic box, and the position of all atoms was always fully relaxed. The same cubic box was used to calculate the energy, geometry, and frequencies of the isolated nitrostyrene molecule.

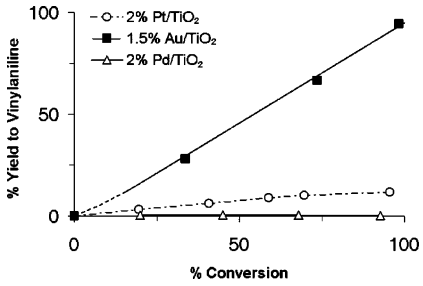

Figure 1. Evolution of yield versus conversion during the 3-nitrostyrene hydrogenation using 2 wt % Pt/TiO_2 (○), 1.5 wt % Au/TiO_2 (■), and 2 wt % Pd/TiO_2 (△).

The TiO_2 (anatase) support was modeled by a (2×2) supercell slab model representing the most stable (001) surface. It contains three TiO_2 layers (nine atomic layers), with the two uppermost TiO_2 layers being also fully relaxed. Finally, Au particles supported on anatase were modeled by a supercell approach in which the anatase slab model unit cell described above was sufficiently enlarged so as to support a Au_{13} particle in such a way that Au particles are kept ∼8 Å apart from each other and there is a vacuum region larger than 15 Å between vertical repeated slabs. In order to stabilize the Au_{13} particle on top of the TiO_2 support, an oxygen vacancy was artificially introduced in the anatase model just below the metallic particle. The largest supercell contains 172 atoms, and calculations require access to a large parallel supercomputer.

All calculations were carried out using the VASP code,[12] with exchange correlation effects being described by the Perdew−Wang (PW91)[13] version of the generalized gradient approximation (GGA). The density was expanded in a plane wave basis set with a 415 eV cutoff for the kinetic energy to represent the valence electron density; a larger cutoff of 515 eV was used in some cases to test the convergence of adsorption energies and geometries with respect to this parameter. The effect of the core electrons in the valence density was taken into account by means of the projected augmented wave (PAW) method.[14] The Brillouin zone of the gold surface unit cells was described with a $3 \times 3 \times 1$ *k*-points grid within the Monkhorst−Pack scheme, while the rest of the calculations (Au_{38} nanoparticle, TiO_2, and Au_{13}/TiO_2) were carried out for the Γ *k*-point. The resulting structures were further characterized as minima by a pertinent frequency analysis calculation. These vibrational frequencies were calculated by diagonalizing the block Hessian matrix corresponding to displacements of the coordinates of all the atoms of nitrostyrene molecule.

Results and Discussion

Catalytic Experiments. Kinetic results in Figure 1 clearly show that, with Au/TiO_2, it is possible to achieve very high chemoselectivity toward the hydrogenation of the nitro group in nitrostyrene (eq 1) when working at levels of conversion close to 100%.

(10) (a) Corma, A.; Concepción, P.; Serna, P. *Angew. Chem., Int. Ed.* **2007**, *46*, 7266−7269. (b) Corma, A.; Serna, P.; García, H. *J. Am. Chem. Soc.* **2007**, *119*, 6358−6359.
(11) (a) Comotti, M.; Della Pina, C.; Matarrese, R.; Rossi, M. *Angew. Chem., Int. Ed.* **2004**, *43*, 5812−5815. (b) Budroni, G.; Corma, A. *Angew. Chem., Int. Ed.* **2007**, *45*, 3328−3331.
(12) (a) Kresse, G.; Furthmüller, J. *Phys. Rev. B* **1996**, *54*, 11169−11186. (b) Kresse, G.; Hafner, J. *Phys. Rev. B* **1993**, *47*, 558−561.
(13) (a) Perdew, J. P.; Chevary, J. A.; Vosko, S. H.; Jackson, K. A.; Pederson, M. R.; Singh, D. J.; Fiolhais, C. *Phys. Rev. B* **1992**, *46*, 6671−6687. (b) Perdew, J. P.; Wang, Y. *Phys. Rev. B* **1992**, *45*, 13244−13249.
(14) Blöchl, P. E. *Phys. Rev. B* **1994**, *50*, 17953−17979.

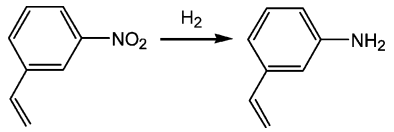

(1)

To explain this result, one can assume, to a first approximation, that the intrinsic rate for the reduction of the nitro group on the gold catalyst is much larger than that of the olefinic group. To check this hypothesis, hydrogenations of nitrobenzene and styrene were carried out separately. Turnover frequency (TOF) values were calculated from initial reaction rates as the number of molecules transformed per hour and per gold atom. The results presented in Table 1 indicate that the TOF for hydrogenating nitrobenzene is 2.2 times larger than that for styrene with the Au/TiO_2 catalyst. In contrast, on both Au/SiO_2 and Pt/TiO_2 catalysts, styrene is hydrogenated more rapidly than nitrobenzene. While these results are consistent with a higher chemoselectivity of the Au/TiO_2 system to hydrogenate a substrate such as 3-nitrostyrene, they cannot explain the 98% chemoselectivity for the hydrogenation of the nitro group on Au/TiO_2. To explain the very high selectivity of gold, a second kinetic factor that may influence selectivity was also considered: that is, the preferential adsorption of the nitro versus the olefinic group when there is competitive adsorption. This hypothesis was tested by studying the reactivity of styrene in the presence of nitrobenzene.

Results in Table 2 indicate that, although styrene hydrogenation can occur on Au/TiO_2, its reaction rate is strongly inhibited by the presence of nitrobenzene, while the hydrogenation of nitrobenzene is practically not influenced by the presence of styrene. Therefore, from the kinetic experiments, one can conclude that the high chemoselectivity observed with Au/TiO_2 not only is due to a higher intrinsic activity for hydrogenating the nitro with respect to the olefinic group but also, especially, is a consequence of the preferential adsorption of nitrostyrene through the nitro group on the Au/TiO_2 catalyst. This conclusion is further supported by *in situ* IR competitive adsorption results. Thus, when nitrobenzene is adsorbed on the TiO_2 support or on the Au/TiO_2 catalyst (Figure 2a), the asymmetric $\nu_{as}(NO_2)$ IR vibration frequency shifts from 1552 cm^{-1} in the gas phase to 1526 cm^{-1}, while no shift for the aromatic ring vibration frequencies (1620, 1606, 1585 cm^{-1}) is observed. This suggests that nitrobenzene interacts with the catalyst through the nitro group. In this case, the support plays an important role, since FTIR measurements of nitrobenzene adsorption on Au/SiO_2 (Figure 2b), in which only the interaction between nitrobenzene and the gold nanoparticles can be observed, indicate that the nitro group adsorbs weakly on metallic gold.

Styrene adsorption on both TiO_2 and Au/TiO_2 samples leads to similar FTIR spectra (Figure 3b). The IR bands at 1601, 1494, and 1450 cm^{-1} are related to the stretching vibrations of the phenyl ring, and the bands at 1630 and 1416 cm^{-1} are attributed to the ν(C═C) and δ(═C—H) vibrations of the vinyl group, respectively. Interestingly, only a very small shift (<5 cm^{-1}) of the IR bands associated with the olefinic groups occurs with respect to the molecule in the gas phase, indicating an even weaker interaction of the double bond with the surface. In other words, when comparing the IR spectroscopy results for the adsorption of nitrobenzene and styrene, it appears quite clear that a stronger adsorption/interaction of the nitro group with respect to the olefinic group on either TiO_2 or Au/TiO_2 occurs.

Table 1. Turnover Frequency of Au/TiO_2, Au/SiO_2, and Pt/TiO_2 Catalysts for the Hydrogenation of Styrene and Nitrobenzene[a]

	TOF (mol converted h^{-1} mol^{-1} metal)	
substrate	styrene	nitrobenzene
1.5% Au/TiO_2	160	365
1.6% Au/SiO_2	110	20
2% Pt/TiO_2	660	200

[a] TiO_2 is shown to play an important role for activating the nitro group in the gold catalysts. In contrast, the platinum sample is shown to be especially active for catalyzing the C═C hydrogenation. Reaction conditions: 120 °C, 9 bar (gold catalysts); 40 °C, 3 bar (platinum catalyst). Feeding (1 mL): 8.5 mol % of substrate, 90.5 mol % of toluene (solvent), and 1 mol % of *o*-xylene (internal standard).

Table 2. Turnover Frequency of the Au/TiO_2 Catalyst for the Hydrogenation of Styrene and Nitrobenzene at Different Feeding Compositions[a]

feeding (mol %)		TOF (mol converted h^{-1} mol^{-1} Au)	
styrene	nitrobenzene	styrene	nitrobenzene
0	8.5	0	365
4.25	4.25	16	405
8.5	0	160	0

[a] While the double-bond reduction rate notably decreases in the presence of a nitro group, this one keeps a very similar reaction rate, independent of the styrene concentration. Reaction conditions: 120 °C, 9 bar. Feeding (1 mL): 8.5 mol % of substrate (styrene + nitrobenzene), 90.5 mol % of toluene (solvent), and 1 mol % of *o*-xylene (internal standard).

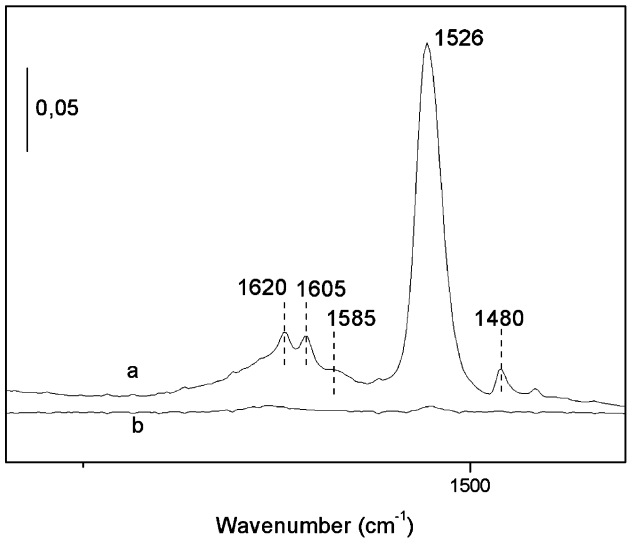

Figure 2. FTIR spectra of nitrobenzene adsorption at 25 °C on (a) Au/TiO_2 and (b) Au/SiO_2.

This is further confirmed by studying the competitive adsorption of nitrobenzene and styrene with a 1:1 molar ratio (Figure 3c). In this case, bands associated with nitrobenzene are exclusively observed, indicating a preferential adsorption of the nitro group from nitrobenzene versus the double bond in the styrene. Finally, FTIR nitrostyrene adsorption experiments on TiO_2 and Au/TiO_2 (Figure 4) show that nitrostyrene adsorbs selectively through the nitro group.

From the FTIR adsorption studies, it can be concluded that (i) both the nitro and the olefinic groups can adsorb on Au/TiO_2, though the interaction through the nitro group is stronger and competes very favorably with the adsorption of the olefinic group, and (ii) the nitro group adsorbs weakly on metallic gold and more strongly on the TiO_2 support.

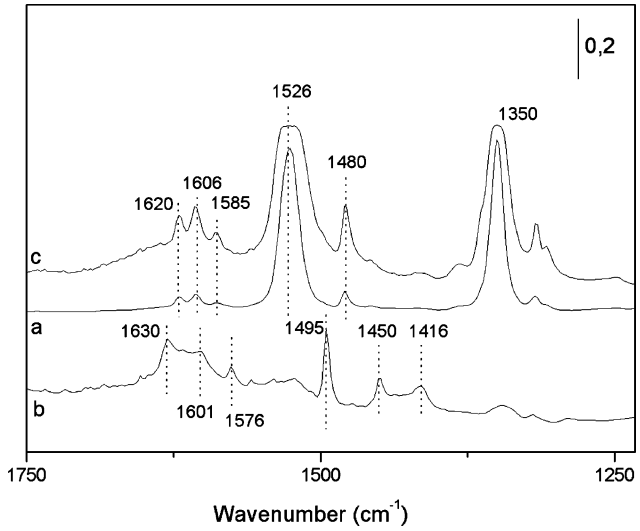

Figure 3. FTIR spectra of adsorption of nitrobenzene (a), nitrostyrene (b), and a mixture of nitrobenzene and styrene with a 1:1 molar ratio (c) at 25 °C on TiO_2 or Au/TiO_2.

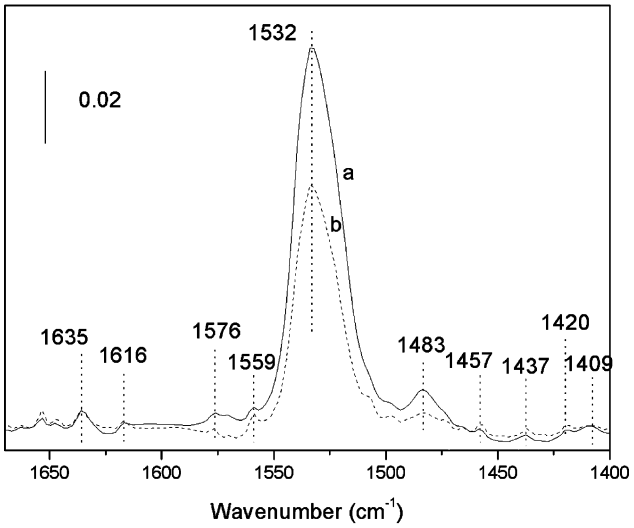

Figure 4. FTIR spectra of nitrostyrene adsorption at 25 °C on (a) Au/TiO_2 and (b) TiO_2.

At this point, and to go one step further toward understanding the molecular interactions at the surface, quantum chemical calculations were performed to model the adsorption of the reactant on different types of gold surfaces, on isolated gold nanoparticles, on the TiO_2 support, and on Ti−O−Au interface sites as described in the previous section. Analysis of the interaction energies, geometry deformation, and vibrational frequencies should allow us to reach definitive conclusions about the nature of the catalyst active sites and the modes of reactant adsorption.

DFT Calculations. 1. Nitrostyrene Adsorption on Gold. The present density functional calculations predict that nitrostyrene interacts weakly with Au(111) and Au(001) surfaces, in agreement with experiment (Au/SiO_2). The calculated adsorption energies are small (Table 3), the adsorbed molecule lies parallel to the Au surface at a distance of ∼3−4 Å (Figure 5), and the optimized N═O and C═C distances are almost identical to those obtained for the isolated molecule in the gas phase. A quite different situation is obtained for the interaction of the nitrostyrene molecule with the low-coordinated Au atoms of the Au_{MAR} model or with the Au_{38} nanoparticle. For the Au_{MAR}, it is found that both the nitro group and the C═C double bond interact moderately with low-coordinated Au atoms situated in the edge of the monatomic row, the calculated adsorption energies being 8.7 and 12.2 kcal mol^{-1}, respectively. The adsorption through the C═C double bond is of π nature, with a concomitant increase of 0.05 Å in the CC bond length. Analysis of the final geometry shows that the main interaction occurs through the C═C double bond, but it also reveals that one of the C atoms of the benzene ring is quite strongly interacting with a Au atom in the monatomic row edge (Figure 6). This coordination provokes a coupling of the different vibrational modes in the 1650−1500 cm^{-1} region, all of them associated with the nitro group and the carbon skeleton of the molecule. As a consequence, the characteristic spectroscopic band at 1638 cm^{-1}, corresponding to the pure C═C stretching mode, shifts to ∼1510 cm^{-1} (Table 4) and includes important contributions from other modes, while the vibrational modes including large contributions from the nitro group appear at 1574 and 1545 cm^{-1}. Adsorption through the nitro group in the same Au_{MAR} model is only 3.5 kcal mol^{-1} less favorable but significantly activates the NO_2 group, since the optimized NO distances are now 0.04 Å larger than the corresponding values for the gas-phase molecule (Table 3). This geometry distortion is large enough to provoke a change in the asymmetric $\nu_{as}(NO_2)$ vibration frequency from 1537 cm^{-1} in the gas phase to ∼1470 cm^{-1} (Table 4) and with significant mixing with the vibrational modes of the aromatic ring, while other modes, clearly dominated by NO contributions, appear at ∼1300 cm^{-1}. Nitrostyrene's interaction with the Au_{38} nanoparticle model is stronger, as reflected by the higher adsorption energies obtained and the larger increase in the N−O and C−C bond lengths (Table 3). Again, the interaction through the C═C double bond is more favorable than the interaction through the nitro group, but both groups appear to be highly activated. In the case of the C═C interaction, the adsorption is of di-σ nature, each of the carbon atoms of the double bond interacts with one Au atom, and the C−C distance increases to 1.47 Å, which is close to the standard value for a C−C single bond. It is important to remark that, as shown in Figure 7, there is also a noticeable distortion of the Au_{38} nanoparticle due to the interaction with some of the C atoms of the benzene ring. As could be expected, the characteristic vibration frequency associated with the C═C stretching mode does not show up simply because, as mentioned above, the carbon−carbon bond changes its character from double- to single-bond. Moreover, the NO_2 group's asymmetric vibration couples with some of the modes associated with the aromatic ring, as in the case of interaction with the Au_{MAR} model, but here two modes dominated by the nitro group's atomic displacements, which appear at 1562 and 1509 cm^{-1}, can be clearly identified. In contrast, interaction of nitrostyrene with the Au_{38} nanoparticle through the NO_2 group results in a significant increase of one of the NO distances to 1.30 Å. Here, the NO_2-related modes, appearing at 1494 and 1439 cm^{-1}, are even more strongly coupled to those of the aromatic ring, the ones clearly dominated by NO motions appearing now at 1395 and 1371 cm^{-1}.

From the results corresponding to the interaction of nitrostyrene with low-coordinated Au atoms, either in the extended Au_{MAR} or in the Au_{38} particle, it can be concluded that both the

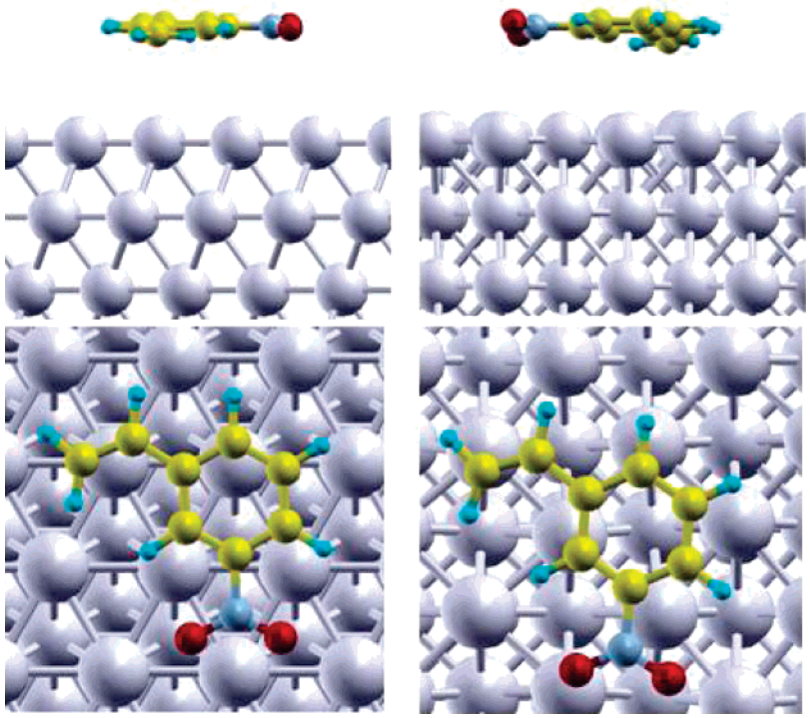

Figure 5. Nitrostyrene adsorption on perfect Au(111) (left) and Au(001) (right) surfaces.

Table 3. Adsorption Energies (kcal/mol) and Optimized Values of the Most Important Distances (Å) of Nitrostyrene Adsorbed on the Different Systems Considered

	E_{ads}	*r*NO	*r*CC	*r*OAu	*r*CAu	*r*OTi
isolated		1.24, 1.24	1.34			
Au(111)	−2.5	1.24, 1.24	1.34	4.09, 4.14	3.61, 3.75	
Au(001)	−2.6	1.24, 1.24	1.35	3.36, 4.04	3.07, 3.52	
Au_{MAR} (NO_2)	−8.7	1.28, 1.28	1.34	2.32, 2.32		
Au_{MAR} (C═C)	−12.2	1.24, 1.24	1.39		2.25, 2.41	
Au_{38} (NO_2)	−20.0	1.30, 1.26	1.34	2.31, 2.53		
Au_{38} (C═C)	−28.9	1.25, 1.24	1.47		2.15, 2.29	
TiO_2 (strongly)	−42.4	1.27, 1.24	1.34			2.14, 2.39
TiO_2 (weakly)	−24.0	1.24, 1.24	1.34			3.71, 4.01
Au_{13}/TiO_2	−15.4	1.39, 1.39	1.34	2.32, 2.33		2.06, 2.14

nitro group and the C═C double bond are activated, but without any preferential activation toward one or the other. Consequently, the preferential adsorption of the nitro group on the gold particle surface cannot explain the chemoselective hydrogenation and the kinetic results presented above. Indeed, when nitrostyrene hydrogenation is carried out on gold supported on an "inert" carrier such as SiO_2, the results presented in Table 5 clearly show that, while active, this catalyst is not selective for the hydrogenation of the nitro group, in agreement with the prediction from the present theoretical study. Taking into account all results reported up to now, we have to consider the possibility that the support, either by itself or through its interaction with the gold nanoparticles, could be responsible for the selective adsorption and reactivity of the nitro groups. Therefore, we have extended the theoretical adsorption studies to supported gold nanoparticles.

2. Nitrostyrene Adsorption on TiO_2 and Au/TiO_2. When nitrostyrene approaches the TiO_2 surface, the C═C interaction with the Ti atoms of the oxide support is possible only if the molecule is parallel to the TiO_2 surface. However, the repulsion between the aromatic ring and the O atoms of the oxide surface is stronger, and all attempts to locate a minimum corresponding to the adsorption through the C═C on TiO_2 evolved to a structure in which the interaction occurs via the nitro group and, more precisely, between the oxygen atoms of the nitro group and the Ti atoms of the surface (Figure 8). In this structure, the molecule lies perpendicular to the surface, with the two O atoms of the nitro group 2.14 and 2.39 Å from the nearest surface Ti atoms, and with a lengthening of one of the N−O bonds from 1.24 to 1.27 Å. The characteristic spectroscopic feature associated with the C═C stretching mode appears at 1641 cm^{-1} (Table 4), and the vibrational modes associated with the nitro group are strongly coupled to those of the aromatic ring and appear at 1484 and 1459 cm^{-1}, far away from the characteristic frequency expected for the nitro group of the isolated molecule. The calculated adsorption energy is quite large, 42 kcal/mol, suggesting that this strongly chemisorbed nitrostyrene molecule might be just a spectator and not the reactive species. Here, it is worth pointing out that the experimental IR measurements, previously described for the interaction of nitrostyrene with the TiO_2 support and the Au/TiO_2 catalyst, show a clear band at 1532 cm^{-1} which, in the light of the present theoretical results, cannot be assigned to nitrostyrene strongly chemisorbed through the nitro group. In order to assign this experimentally observed band, several geometry optimization calculations were carried out, starting from a variety of conformations. In this way, a

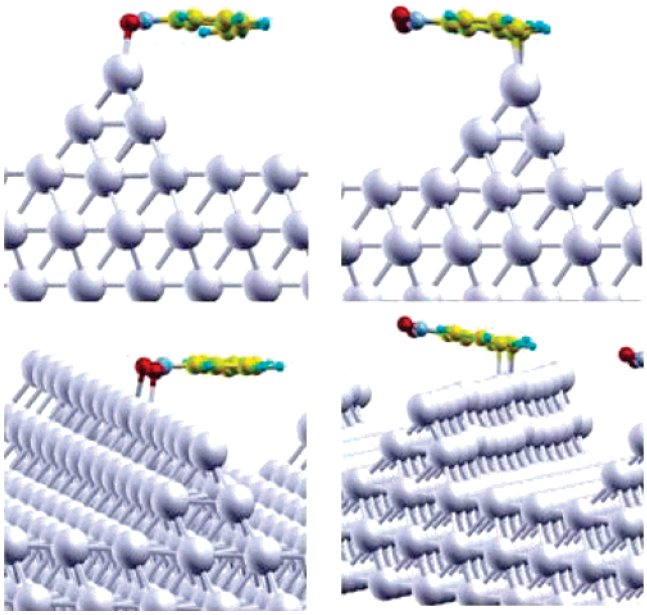

Figure 6. Nitrostyrene adsorption on the edge of a monatomic row on a Au(111) surface through the nitro group (left) and the C═C double bond (right).

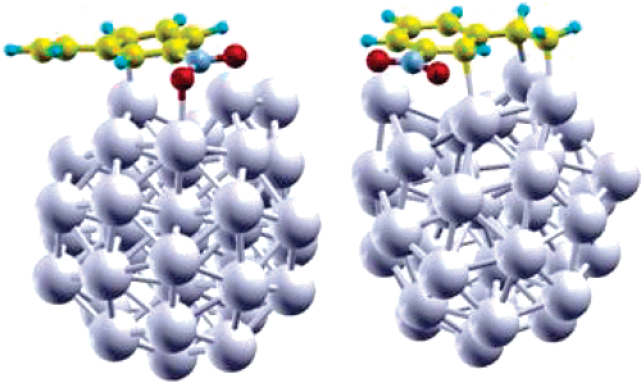

Figure 7. Nitrostyrene adsorption on a Au_{38} nanoparticle through the nitro group (left) and the C═C double bond (right).

Table 4. Calculated Vibrational Frequencies (cm^{-1}) of Nitrostyrene Adsorbed on the Different Systems Considered

	νCC	νNO_2+O	νNO_2
isolated	1638	1537	1317
Au_{MAR} (NO_2)	1636	1470	1308, 1299
Au_{MAR} (C═C)	1516, 1509	1574, 1545	
Au_{38} (NO_2)	1627	1494, 1439	1395, 1371
Au_{38} (C═C)		1562, 1509	
TiO_2 (strongly)	1641	1484, 1459	1281, 1268
TiO_2 (weakly)	1639	1524	1319
Au_{13}/TiO_2	1640		1227, 1138

new adsorption complex was obtained in which nitrostyrene is weakly bonded to the TiO_2 surface. The calculated adsorption energy is 24 kcal/mol (Table 3), the distances from the O atoms of the nitro group to the nearest surface Ti atoms are larger than 3.7 Å, and the NO distances are only slightly elongated with respect to those obtained for the isolated molecule. As a consequence of these small changes in the molecular geometry, the asymmetric $\nu_{as}(NO_2)$ vibration frequency shifts from 1537 cm^{-1} in the gas phase to 1524 cm^{-1} (Table 4). The good agreement between the calculated and the experimentally measured $\Delta\nu_{as}(NO_2)$ frequency shifts (−13 and −19 cm^{-1}, respectively) suggests that the nitrostyrene molecules observed by IR spectroscopy are precisely those weakly adsorbed on the TiO_2 support. Moreover, it further validates the present computational approach and reinforces the conclusions described above for the interaction of nitrostyrene with low-coordinated Au atoms.

The model calculations described so far indicate that, on one hand, interaction of nitrostyrene with pure Au cannot explain the preference for the nitro group activation observed in the catalytic experiments and, on the other hand, the support itself plays only a marginal role in sticking the molecule to the surface. We are left with the possibility that the adsorption can occur on the gold atoms interacting with the support. To analyze this possibility, the adsorption of nitrostyrene on a more realistic model of the catalyst, involving a gold nanoparticle supported on TiO_2, has been studied (Figure 9). Nitrostyrene was situated perpendicular to the TiO_2 surface, at the interface between the gold nanoparticle and the oxide support. In this case, and as described above, a strong interaction between the O atoms of the nitro group and the Ti atoms of the support is observed, with calculated Ti−O distances of 2.06 and 2.14 Å. However, for the Au/TiO_2 system, there is another noticeable interaction between the O atoms of the nitro group and two Au atoms at the nanoparticle edge. Interestingly enough, these are low-coordinated Au atoms, directly bonded to four or five other Au atoms, and at 2.6−2.7 Å from an O atom of the support. The calculated adsorption energy at this site is 15.4 kcal/mol, considerably smaller than that on the extended TiO_2 support, and almost as large as that obtained for the interaction of nitrostyrene with the isolated nanoparticles. However, there are two important differences between these two cases. First, the interaction of nitrostyrene with the isolated Au_{38} nanoparticle induces a large distortion of the metallic particle, but it does not modify the geometry of the Au_{13} supported cluster. Second, and most importantly, nitrostyrene adsorption on the Au_{13}-on-TiO_2 supported model strongly activates the nitro group while leaving the C═C almost unaffected. Both NO bond lengths increase to 1.39 Å, and the conformation of the N atom displays a noticeable distortion from planarity, evidenced by the C−N−O−O dihedral angle, which switches from 180° to 125°. Unsurprisingly, the calculated frequency associated with the pure C═C stretching vibrational mode appears at 1640 cm^{-1} (Table 4), while the frequencies dominated by the nitro group atomic displacements are shifted to 1227 and 1138 cm^{-1} and include large contributions from modes related to the aromatic ring vibrations. In other words, the model calculations strongly suggest that, while nitrostyrene can be adsorbed and activated through either the NO_2 or the C═C groups on isolated gold nanoparticles, a different situation appears when this molecule interacts with Au nanoparticles supported on TiO_2. In fact, in this latter situation, selective adsorption and proper activation of the nitro group appear to occur naturally, with the nitro group oxygen atoms interacting with two low-coordinated Au atoms located at the nanoparticle edge in contact with the support. This very selective adsorption and activation on the Au/TiO_2 with respect to isolated Au nanoparticles or with respect to Au/SiO_2 catalysts can explain the high chemoselectivity observed for that catalyst. This is further confirmed by additional catalytic experiments carried out for 3-nitrostyrene hydrogenation using

Table 5. Catalytic Behavior of Different Supported Gold Materials in the Hydrogenation of 3-Nitrostyrene[a]

catalysts	particle size (nm)[b]	amount of catalyst (mg)	TOF[c]	conversion (%), time (h)	selectivity(%) NBE	ABS	ABE	AZO	AZOXY
1.5% Au/TiO_2	3.6	25	173	98.5, 6	0.5	96		3	0.5
4.5% Au/Fe_2O_3	3.5	20	23	25, 2		95		2	3
1.6% Au/SiO_2	4.0	25	10	25, 5	10	30	50		
1.5% Au/C	4.1	25	6	5, 6	17	41	42		

[a] Metal oxides such as TiO_2 and Fe_2O_3 play an important role for preferentially reducing the nitro group, which cannot be achieved by using "inert" supports such as SiO_2 or C. Feeding (1 mL): 8.5 mol % of nitrostyrene, 90.5 mol % of toluene (solvent), and 1 mol % of *o*-xylene (internal standard). NBE, 3-nitroethylbenzene; ABS, 3-aminostyrene; ABE, 3-aminoethylbenzene; AZO, azostyrene; AZOXY, azoxystyrene. [b] Averaged values. [c] Calculated at initial reaction rate as moles of substrate converted per hour and per mole of Au.

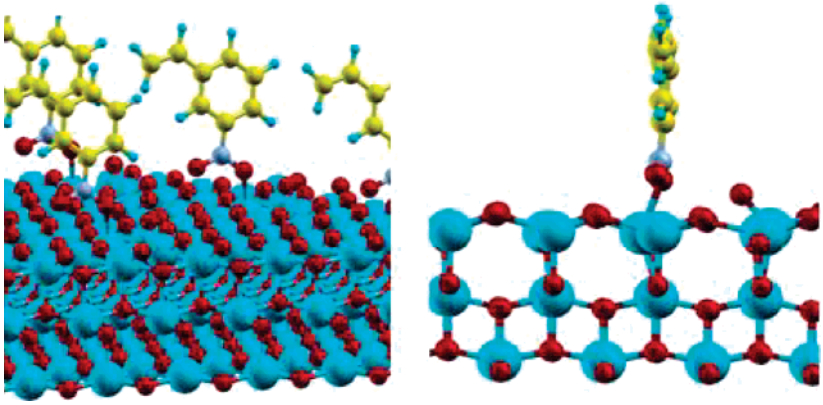

Figure 8. Nitrostyrene adsorption on the TiO_2 support.

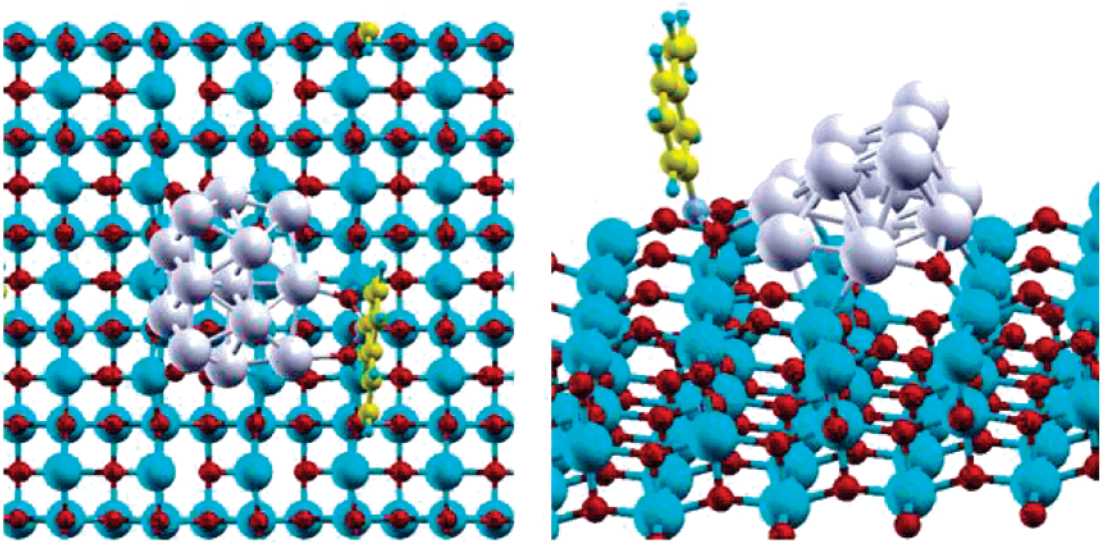

Figure 9. Nitrostyrene adsorption on the Au/TiO_2 catalyst model.

different supports; a summary of the results is shown in Table 5. In agreement with the theoretical study, active supports such as TiO_2 or Fe_2O_3 lead to selective processes, whereas "inert" ones such as SiO_2 or C produce both the reduction of the double bond and the nitro functions.

Conclusions

The high chemoselectivity of Au/TiO_2 for the hydrogenation of substituted nitroaromatics to the corresponding anilines, and more specifically that of nitrostyrene, is due not only to an intrinsic higher rate for the hydrogenation of the nitro versus the olefinic group on the gold catalyst, but also to the very favorable adsorption through the nitro when both groups are competing.

In the most selective Au/TiO_2 catalyst, H_2 is dissociated on gold while nitrostyrene is weakly adsorbed on metallic gold and more strongly on highly uncoordinated gold atoms. Although nitrostyrene adsorbs very strongly and selectively through the nitro group on Ti, the high heat of adsorption (42 $kcal \cdot mol^{-1}$) indicates that the molecules strongly adsorbed on TiO_2 may be spectators. On the other hand, nitrostyrene adsorbs very selectively through the nitro group on two low-coordinated Au atoms at the nanoparticle edge bonded to four or five other

Au atoms and at 2.6−2.7 Å away from an oxygen atom of the support. In this case, the calculated heat of adsorption (15.4 $kcal \cdot mol^{-1}$) and the activation of the NO_2 group strongly favor the reactivity of the adsorbed molecule.

Acknowledgment. We thank the Spanish government (projects MAT2006-14274-C02-01, CTQ2005-08459-CO2-01, UNBA05-33-001, and grant FPU AP2003-4635) and the Generalitat de Catalunya (2005SGR00697, 2005 PEIR 0051/69, and Distinció per a la Promoció de la Recerca Universitaria of F.I.) for financial support. The authors thankfully acknowledge the computer resources, technical expertise, and assistance provided by the Barcelona Supercomputing Center−Centro Nacional de Supercomputación.

JA076721G